Chapter 5

# Unsteady Peristaltic Transport of a Particle–Fluid Suspension: Application to oesophageal swallowing

## 5.1 Introduction

Peristalsis is a pumping mechanism by which a fluid can be transported through a tube/channel when contraction or expansion waves propagate along the tube wall. Most of the physiological fluids in humans or animals are propelled by continuous periodic muscular contractions and expansions of the ducts through which the fluids pass. Peristaltic pumping is involved in swallowing of food bolus through the oesophagus, embryo transport in the uterus, vasomotion of blood vessels, spermatic flows in the male reproductive tracts, transport of urine through the ureter, and also in some other engineering applications. The principle of peristalsis is used to design blood pump in heart lung machines, diabetic pump and roller pumps. Numerous investigations (Shapiro et al., 1969; Li and Brasseur, 1993; Misra and Pandey, 2001; Hayat et al., 2002; Hariharan et al., 2008; Vajravelu et al., 2012; Ellahi et al., 2014; Nadeem et al., 2014) over several years have thrown light on peristalsis but it is still desirable to investigate it in new perspectives.

Study of the theory of particle-fluid mixture is immensely useful for understanding a number of physical phenomena including transportation of solid particles by liquids, mixing operations, particulate suspension theory of blood, flow of food suspension through oesophagus and intestines, urine flow through the ureters, transportation of liquid slurries in chemical and nuclear processing etc. Several industrial food processes involve flow of food

The contents of this chapter are published in Z. Naturforsch. A. 73(2018) 1143-1156.

suspension in which the knowledge of flow properties is essential for assessing pumping requirements. Hung and Brown (1976) investigated various geometric and dynamic effects on peristaltic transport of suspended solid particles in a fluid in a two-dimensional channel. Drew (1979; 1983) presented a two-phase flow model that accounts for a mixture of dispersed small particles in a fluid as the working medium. Srivastava and Srivastava (1989) applied Drew's model (1979) to a particle-fluid mixture flowing in a channel and obtained perturbation solution which satisfies the momentum equations for the case in which amplitude ratio is small. The flow of diseased urine modelled as particle-fluid suspension through the ureters was subsequently studied by Misra and Pandey (1994) who concluded that the mean flow induced by peristaltic motion is proportional to the square of the amplitude ratio and depends on the mean pressure gradient. Ureters are muscular ducts that propel urine from the kidneys to the bladder by peristalsis. Jimenez-Lozano et al. (2011) also presented a model for peristaltic flow in ureters due to a solitary wave with the objective of explaining the flow mechanics of a particle-fluid mixture. Mekheimer and Abdelmaboud (2008) theoretically analyzed peristaltic flow through a uniform and non-uniform annulus filled with particle-fluid suspension by long wavelength approximation. Popularity of the Drew's model is revealed through a series of recent publications in biomechanics involving peristalsis (Bhatti and Zeeshan, 2016a; Bhatti et al., 2016; Bhatti et al., 2017a; Zeeshan et al., 2017; Bhatti et al., 2017b; Bhatti et al., 2018) and rheological flow of blood (Bhatti et al., 2016b; Zeeshan et al., 2018).

The digestive system is accountable for carrying out the food bolus from the mouth to the large intestine. In the oesophageal deglutition, food is ingested through the mouth and when swallowed passes into the pharynx which forces the food bolus rapidly into the oesophagus. This process ends with the transport of the bolus to the stomach by peristaltic contractions of the oesophageal wall. There are several food stuffs which are in the form of particulate suspensions in which the continuous phase is an aqueous solution. Examples are pasta products in sauces, yogurts with fruits, fruit preserves with seeds, vegetable soups, fruit in syrup, sugarcane juice with kiwifruit and many others homemade food items (Martinez-Padilla, 2009). Generally, some of these food items have non-Newtonian behaviour but if the volume fraction of suspended particles is small then they behave as a Newtonian fluid. Moreover, any solid edible item is first masticated with teeth to break into very small

particles, is mixed with saliva or some liquid such as water which can drag into the abdomen through the oesophagus without harming it. What are the implications of the dragged solid particles from medical point of view is another aspect of the investigation. Hence study of particle-fluid suspension is extremely important in relation to oesophageal swallowing. Suspensions are defined as heterogeneous or homogeneous material, in which rigid or deformable particles are suspended in a liquid. Oesophageal swallowing of food suspensions is a two-phase flow model. This model is most appropriate if the dispersed particle phase behaves as continuum. The continuum theory of mixtures is also applicable to hydrodynamics of some biological systems.

Many solutions of peristaltic flows with various approximations are present in the literature. Authors (Shapiro et al., 1969; Li and Brasseur, 1993; Misra and Pandey, 2001) solved problems by using long wavelengths at low Reynolds number approximation in infinite and finite length tubes in which wave number (ratio of tube radius to wavelength) and Reynolds number tend to zero. Pandey et al. (2017) analyzed variation of pressure from the cervical to the distal end of the oesophagus during swallowing with these approximations. The novelty of the investigation lies in the fact that it theoretically discovered the reason for the pressure rise in the distal part of the oesophagus reported by Kahrilas et al. (1995) by using the anatomical measurements reported by Xia et al. (2009). The conclusion they drew was that the wave-amplitude increases progressively as the bolus is swallowed. With this idea Pandey and Tiwari (2017) investigated oesophageal swallowing for the Casson fluid.

Achalasia is a dysfunction that causes inadequate lower sphincter relaxation of oesophagus. As a consequence of it oesophageal clearance is hindered. A possible treatment for patients to overcome this is by application of drugs or operation (Spechler and Castell, 2001). This analysis is also planned to look for finding alternative or supportive ways for a remedial measure.

In a two phase flow like this, a particulate matter suspension, which cannot move itself, is dragged by the fluid mixed with this. Since the two phases will have different velocities, there are several queries to investigate such as which one leads, which one lags behind, what is the mutual relation in the middle of the tube, whether it is different near the tubular boundary etc.

In light of the literature presented above and the discussion that followed, we aim to model swallowing of particulate suspension in a Newtonian fluid through oesophagus in order to investigate the impact of the presence and concentration of suspended particles in the food.

The entire analysis is in dimensionless quantities. We use a regular perturbation method in terms of the wave number for oesophageal swallowing in which the wave number is small but not zero. Flow variables are presented in power series of the wave number to obtain closed form solution up to the first order. Since the wave number is very small and the higher order equations are very much involved, no further analyses will be carried out. The velocities of the two phases will be deduced separately. Pressure equation will also be formulated. The interrelation of the two phases as well as the influence of the particle volume fraction is to be investigated.

## 5.2 Mathematical formulation

We consider oesophagus as a circular cylindrical tube of finite length. The geometrical form of the peristaltic wave in oesophageal wall was given by Li and Brasseur (1993) and modified by Misra and Pandey (2001). The observation of high pressure zone in lower part of oesophagus by Kahrilas et al. (1995) motivated Pandey et al. (2017), in view of the experimental reports of Xia et al. (2009), to reformulate the wall equation with dilating wave amplitude as

$$H'(x',t') = a - \emptyset' e^{k'x'} \cos^2 \frac{\pi}{\lambda}(x' - ct'), \tag{5.1}$$

where $H', x', t', a, \emptyset', k', \lambda$ and $c$ are the radial distance of wall, axial coordinate, time, radius of the tube, amplitude of the wave, amplitude dilation parameter, wavelength and wave velocity respectively (Fig. 5.1).

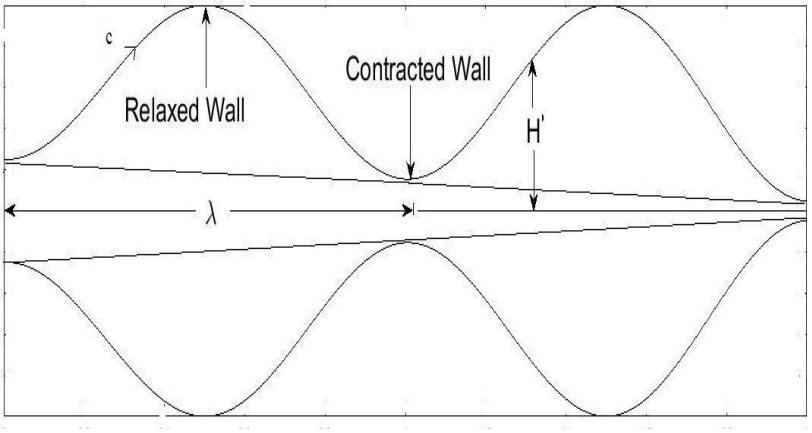


***Fig. 5.1*** *The schematic diagram of wall positions of oesophagus when a peristaltic wave of slightly dilating amplitude propagates along it with velocity c.*

The governing equations are taken in the form of two sets of continuity and momentum equations, one each meant for the fluid and the particulate phase based on the two–phase model of Drew (1979). The governing equations for the fluid and particle phases in the axisymmetric cylindrical coordinates are as follows:

*Fluid phase*:

$$\frac{1}{r'}\frac{\partial((1-C)r'v'_f)}{\partial r'}+\frac{\partial((1-C)u'_f)}{\partial x'}=0, \tag{5.2}$$

$$(1-C)\rho_f\left(\frac{\partial v'_f}{\partial t'}+v'_f\frac{\partial v'_f}{\partial r'}+u'_f\frac{\partial v'_f}{\partial x'}\right)=-(1-C)\frac{\partial p'}{\partial r'}+(1-C)\mu_s(C)\left\{\frac{\partial}{\partial r'}\left(\frac{1}{r'}\frac{\partial(r'v'_f)}{\partial r'}\right)+\frac{\partial^2 v'_f}{\partial x'^2}\right\}$$
$$+CS(v'_p-v'_f), \tag{5.3}$$

$$(1-C)\rho_f\left(\frac{\partial u'_f}{\partial t'}+v'_f\frac{\partial u'_f}{\partial r'}+u'_f\frac{\partial u'_f}{\partial x'}\right)=-(1-C)\frac{\partial p'}{\partial x'}+(1-C)\mu_s(C)\left\{\frac{1}{r'}\frac{\partial}{\partial r'}\left(r'\frac{\partial u'_f}{\partial r'}\right)+\frac{\partial^2 u'_f}{\partial x'^2}\right\}$$
$$+CS(u'_p-u'_f), \tag{5.4}$$

*Particle phase*:

$$\frac{1}{r'}\frac{\partial(Cr'v'_p)}{\partial r'}+\frac{\partial(Cu'_p)}{\partial x'}=0, \tag{5.5}$$

$$C\rho_p\left(\frac{\partial v'_p}{\partial t'}+v'_p\frac{\partial v'_p}{\partial r'}+u'_p\frac{\partial v'_p}{\partial x'}\right)=-C\frac{\partial p'}{\partial r'}+CS(v'_f-v'_p), \tag{5.6}$$

$$C\rho_p\left(\frac{\partial u'_p}{\partial t'}+v'_p\frac{\partial u'_p}{\partial r'}+u'_p\frac{\partial u'_p}{\partial x'}\right)=-C\frac{\partial p'}{\partial x'}+\ CS(u'_f-u'_p), \tag{5.7}$$

where $u'_f, v'_f, u'_p, v'_p,\ \rho_f, \rho_p, C, (1-C)\rho_f, C\rho_p, p, S$ and $\mu_s(C)$ respectively represent axial velocity of the fluid phase, radial velocity of the fluid phase, axial velocity of the particle phase, radial velocity of the particle phase, actual density of the fluid, actual density of the particle material, volume fraction of the particles in the mixture, fluid phase density, particle phase density, pressure, drag coefficient of interaction for the force exerted by one phase on the other and the effective viscosity of suspension. For the present problem, the Stokes drag coefficient for a small particle at low Reynolds number, $S=\frac{9\mu_0}{4r_p^2}$, and Einstein's formula, $\mu_s=\mu_0\mu_r$, shall be used, where $\mu_0$ is the fluid viscosity, $r_p$ is the particle radius and $\mu_r(C)=1+\frac{5C}{2}$ (Drew, 1979).

The following dimensionless parameters are now introduced into the analysis:

$$\left.\begin{array}{l} x=\frac{x'}{\lambda},\quad r=\frac{r'}{a},\quad t=\frac{ct'}{\lambda}\ ,\ h=\frac{H'}{a},\ k=k'\lambda,\ u_f=\frac{u'_f}{c},\\ u_p=\frac{u'_p}{c},\ v_f=\frac{v'_f}{c\delta},\ \delta=\frac{a}{\lambda},\ v_p=\frac{v'_p}{c\delta}\ ,\ Q=\frac{Q'}{\pi a^2 c},\quad \rho=\frac{\rho_p}{\rho_f},\\ \emptyset=\frac{\emptyset'}{a}\ ,\ p=\frac{p'a\delta}{\mu_s c},\quad Re_0=\frac{\rho_f ca}{\mu_0},\ Re=\delta\,Re_0,\ M=\frac{9}{4}\left(\frac{a}{r_p}\right)^2, \end{array}\right\} \tag{5.8}$$

where $\delta, Re_0, Re,\ and\ M$ are respectively the wave number, the Reynolds number, the modified Reynolds number and the drag parameter. Introduced dimensionless quantities reduce the wall equation (5.1) and governing equations (5.2)-(5.7) to

$$h(x,t)=1-\emptyset e^{kx}\cos^2\pi(x-t)\ . \tag{5.9}$$

$$\frac{1}{r}\frac{\partial((1-C)rv_f)}{\partial r}+\frac{\partial((1-C)u_f)}{\partial x}=0, \tag{5.10}$$

$$\delta^3(1-C)Re_0\left(\frac{\partial v_f}{\partial t}+v_f\frac{\partial v_f}{\partial r}+u_f\frac{\partial v_f}{\partial x}\right)=-\mu_r(1-C)\frac{\partial p}{\partial r}+\mu_r(1-C)\left\{\delta^2\frac{\partial}{\partial r}\left(\frac{1}{r}\frac{\partial(rv_f)}{\partial r}\right)+\delta^4\frac{\partial^2 v_f}{\partial x^2}\right\}+\delta^2\,CM(v_p-v_f), \tag{5.11}$$

$$\delta(1-C)Re_0\left(\frac{\partial u_f}{\partial t}+v_f\frac{\partial u_f}{\partial r}+u_f\frac{\partial u_f}{\partial x}\right)=-\mu_r(1-C)\frac{\partial p}{\partial x}+\mu_r(1-C)\left\{\frac{1}{r}\frac{\partial}{\partial r}\left(r\frac{\partial u_f}{\partial r}\right)+\delta^2\frac{\partial^2 u_f}{\partial x^2}\right\}$$

$$+CM(u_p-u_f), \tag{5.12}$$

$$\frac{1}{r}\frac{\partial(Crv_p)}{\partial r}+\frac{\partial(Cu_p)}{\partial x}=0, \tag{5.13}$$

$$\rho\delta^3 CRe_0\left(\frac{\partial v_p}{\partial t}+v_p\frac{\partial v_p}{\partial r}+u_p\frac{\partial v_p}{\partial x}\right)=-\mu_r C\frac{\partial p}{\partial r}+\delta^2 CM(v_f-v_p), \tag{5.14}$$

$$\rho\delta CRe_0\left(\frac{\partial u_p}{\partial t}+v_p\frac{\partial u_p}{\partial r}+u_p\frac{\partial u_p}{\partial x}\right)=-\mu_r C\frac{\partial p}{\partial x}+\ CM(u_f-u_p). \tag{5.15}$$

Boundary conditions are essential requirements for obtaining solution of a system of differential equations. However, in a practical problem such as one undertaken here, physics of fluid and solid particles have to be properly taken into consideration. For instance, no solid particle can stick to a solid boundary, else the definition of rigidity will be violated. In fact, it is dragged by the fluid which can stick to the boundary. Hence we cannot impose no-slip condition on solid particles at the boundary of the tubular wall. The dimensionless boundary conditions, to be imposed on the fluid molecules and the solid particles for the sake of solution may be put as follows:

$$\left.\begin{aligned} u_f\big|_{r=h}=0,\ \ \frac{\partial u_f}{\partial r}\Big|_{r=0}=0,\ \ v_f\big|_{r=0}=0,\ \ v_f\big|_{r=h}=\frac{\partial h}{\partial t},\\ \frac{\partial u_p}{\partial r}\Big|_{r=0}=0\,,\quad v_p\big|_{r=0}=0. \end{aligned}\right\} \tag{5.16}$$

## 5.3 Perturbation solution

To solve the problem, a regular perturbation expansion in terms of wave number, $\delta$ ($\ll 1$), is used and assumed that particle volume fraction, $C$, is low and is of the form $C=\delta C^{(1)}$. We consider the solutions for the fluid and particle velocities and the pressure of the form

$$u_f(r,x,t)=u_f{}^{(0)}+\delta u_f{}^{(1)}+O(\delta^2), \tag{5.17}$$

$$v_f(r,x,t)=v_f{}^{(0)}+\delta v_f{}^{(1)}+O(\delta^2), \tag{5.18}$$

$$u_p(r,x,t)=u_p{}^{(0)}+\delta u_p{}^{(1)}+O(\delta^2), \tag{5.19}$$

$$v_p(r,x,t) = {v_p}^{(0)} + \delta {v_p}^{(1)} + O(\delta^2), \tag{5.20}$$

$$p(r,x,t) = p^{(0)} + \delta p^{(1)} + O(\delta^2). \tag{5.21}$$

Substituting these expansions in Eqs. (5.10)-(5.15), and comparing the coefficients of like powers of $\delta$, we get a set of linear differential equations as given below.

The zero[th]-order system, i.e., coefficients of $\delta^0$ equated on the two sides, is

$$\frac{1}{r}\frac{\partial(r{v_f}^{(0)})}{\partial r} + \frac{\partial {u_f}^{(0)}}{\partial x} = 0, \tag{5.22}$$

$$\frac{\partial p^{(0)}}{\partial r} = 0, \tag{5.23}$$

$$\frac{\partial p^{(0)}}{\partial x} = \frac{1}{r}\frac{\partial}{\partial r}\left(r\frac{\partial {u_f}^{(0)}}{\partial r}\right), \tag{5.24}$$

subject to the boundary conditions:

$$\left.\frac{\partial {u_f}^{(0)}}{\partial r}\right|_{r=0} = 0, \;\; \left.{u_f}^{(0)}\right|_{r=h} = 0, \;\; \left.{v_f}^{(0)}\right|_{r=0} = 0, \left.{v_f}^{(0)}\right|_{r=h} = \frac{\partial h}{\partial t}. \tag{5.25}$$

The first-order system, i.e., coefficients of $\delta$ equated on the two sides, is

$$\frac{1}{r}\frac{\partial(r{v_f}^{(1)})}{\partial r} + \frac{\partial {u_f}^{(1)}}{\partial x} = 0, \tag{5.26}$$

$$\frac{\partial p^{(1)}}{\partial r} = 0, \tag{5.27}$$

$$Re_0\left(\frac{\partial {u_f}^{(0)}}{\partial t} + {v_f}^{(0)}\frac{\partial {u_f}^{(0)}}{\partial r} + {u_f}^{(0)}\frac{\partial {u_f}^{(0)}}{\partial x}\right) = -\frac{\partial p^{(1)}}{\partial x} - \frac{3C^{(1)}}{2}\frac{\partial p^{(0)}}{\partial x} + \frac{3C^{(1)}}{2}\frac{1}{r}\frac{\partial}{\partial r}\left(r\frac{\partial {u_f}^{(0)}}{\partial r}\right) + \frac{1}{r}\frac{\partial}{\partial r}\left(r\frac{\partial {u_f}^{(1)}}{\partial r}\right) + MC^{(1)}({u_p}^{(0)} - {u_f}^{(0)}), \tag{5.28}$$

$$C^{(1)}\left(\frac{1}{r}\frac{\partial(r{v_p}^{(0)})}{\partial r} + \frac{\partial {u_p}^{(0)}}{\partial x}\right) = 0, \tag{5.29}$$

$$C^{(1)}\frac{\partial p^{(0)}}{\partial r} = 0, \tag{5.30}$$

$$C^{(1)}\frac{\partial p^{(0)}}{\partial x} = MC^{(1)}({u_f}^{(0)} - {u_p}^{(0)}), \tag{5.31}$$

subject to the boundary conditions:

$$v_p{}^{(0)}\big|_{r=h} = 0,\ \left.\frac{\partial u_f{}^{(1)}}{\partial r}\right|_{r=0} = 0,\ u_f{}^{(1)}\big|_{r=h} = 0,\ \left.\frac{\partial u_p{}^{(0)}}{\partial r}\right|_{r=0} = 0,\ v_f{}^{(1)}\big|_{r=0} = 0. \tag{5.32}$$

We need to express analytical results in terms of time-averaged volume flow rate which is defined as $\bar{Q}(x) = \int_0^1 Q(x,t)dt$, with the volume flow rate as a sum of that for the two phases, i.e.,

$$Q(x,t) = Q_f(x,t) + Q_p(x,t), \tag{5.33}$$

where $Q_f(x,t) = 2\int_0^h (1-C)u_f r dr$ and $Q_p(x,t) = 2\int_0^h C u_p r dr$ are the instantaneous volume flow rates for the fluid and particle phases respectively. It is a tedious job due to several involved expressions. Hence, in order to avoid complicacies, we use the transformations from the unsteady laboratory frame to steady wave frame for this purpose only. All the other analyses will be later, from the section 5.3.1 onwards, carried out once again in the unsteady laboratory frame.

The wave frame parameters, given on the left side of the equality sign, are related to the corresponding parameters in the laboratory frame, given on the right side, in the non-dimensional form by

$$\left.\begin{aligned} X = x - t,\ \ R = r,\ \ U_i(R,X) = u_i(r,x,t) - 1, \\ V_i(R,X) = v_i(x,r,t),\ \ q = Q(x,t) - h^2, \end{aligned}\right\} \tag{5.34}$$

where $(R,X)$, $(V_i,U_i)$ and $q$ are respectively the coordinate system, the velocity field ($i = f,p$) and the flow rate in the wave frame.

In view of (34), $\overline{Q}(x) = q + \int_0^1 h^2 dt$, and hence

$$q = Q(x,t) - h^2 = \bar{Q}(x) - 1 + \emptyset\, e^{kx} - \tfrac{3}{8}\,\emptyset^2 e^{2kx}. \tag{5.35}$$

The regular perturbation expansions for $Q$ and $\bar{Q}$ are respectively $Q = Q^{(0)} + \delta Q^{(1)} + O(\delta^2)$ and $\overline{Q} = \bar{Q}^{(0)} + \delta\bar{Q}^{(1)} + O(\delta^2)$.

### 5.3.1 Solution of the zero$^{th}$-order system

Integrating Eq. (5.24) with respect to $r$, in view of Eq. (5.23), and using the first boundary condition of Eq. (5.25), we get

$$\frac{\partial u_f^{(0)}}{\partial r} = \frac{\partial p^{(0)}}{\partial x}\frac{r}{2},$$

which, on integrating once more with respect to $r$ and using the second boundary condition of Eq. (5.25), gives

$$u_f^{(0)} = \frac{1}{4}\frac{\partial p^{(0)}}{\partial x}(r^2 - h^2). \tag{5.36}$$

Solving continuity equation (5.22) together with Eq. (5.36) and using the third boundary condition of Eq. (5.25), it yields

$$v_f^{(0)} = \frac{r}{4}\left\{h\frac{\partial h}{\partial x}\frac{\partial p^{(0)}}{\partial x} - \frac{\partial^2 p^{(0)}}{\partial x^2}\left(\frac{r^2}{4} - \frac{h^2}{2}\right)\right\}. \tag{5.37}$$

Now applying the fourth boundary condition of (5.25) in Eq. (5.37) and simplifying, we get

$$\frac{h^3}{16}\frac{\partial^2 p^{(0)}}{\partial x^2} + \frac{h^2}{4}\frac{\partial h}{\partial x}\frac{\partial p^{(0)}}{\partial x} = \frac{\partial h}{\partial t},$$

from which, the zero$^{th}$ order pressure gradient is derived as

$$\frac{\partial p^{(0)}}{\partial x} = \frac{g(t)+16\int_0^x h(s,t)\frac{\partial h(s,t)}{\partial t}ds}{h^4}, \tag{5.38}$$

where $g(t)$ is an arbitrary function of $t$.

Therefore, zero$^{th}$ order pressure at an arbitrary point along the length of the oesophagus is given by

$$p^{(0)}(x,t) = p^{(0)}(0,t) + \int_0^x \frac{g(t)+16\int_0^{x_1} h(s,t)\frac{\partial h(s,t)}{\partial t}ds}{h^4(x_1,t)}dx_1 . \tag{5.39}$$

The arbitrary function $g(t)$ may be evaluated by putting $x = l$ in Eq. (5.39) as

$$g(t) = \left\{ p^{(0)}(l,t) - p^{(0)}(0,t) + 16 \int_0^l \frac{\int_0^{x_1} h(s,t) \frac{\partial h(s,t)}{\partial t} ds}{h^4(x_1,t)} dx_1 \right\} \left\{ \int_0^l \frac{1}{h^4(x_1,t)} dx_1 \right\}^{-1}. \tag{5.40}$$

Further, the zero[th] order flow rate, in view of Eq. (5.33), may be given by

$$Q^{(0)} = Q_f^{(0)} + Q_p^{(0)} = 2 \int_0^h u_f{}^{(0)} r dr + 0 = -\frac{1}{8} \frac{\partial p^{(0)}}{\partial x} h^4.$$

Note that, in view of Eq. (5.35), we have $Q^{(0)} = \bar{Q}^{(0)} - 1 + \emptyset\, e^{kx} - \frac{3}{8}\, \emptyset^2 e^{2kx} + h^2$. Therefore,

$$\frac{\partial p^{(0)}}{\partial x} = -8 \left\{ \frac{\bar{Q}^{(0)} - 1 + \emptyset\, e^{kx} - \frac{3}{8} \emptyset^2 e^{2kx} + h^2}{h^4} \right\} = P_0 \ \ (say). \tag{5.41}$$

Hence, from Eqs. (5.36), (5.37) and (5.41), the zero[th] order axial and radial velocities of the fluid, in terms of zero[th] order time-averaged volume flow rate, are given by

$$u_f{}^{(0)} = \frac{P_0}{4} (r^2 - h^2). \tag{5.42}$$

$$v_f{}^{(0)} = \frac{r}{4} \left\{ h \frac{\partial h}{\partial x} P_0 - \frac{\partial P_0}{\partial x} \left( \frac{r^2}{4} - \frac{h^2}{2} \right) \right\}. \tag{5.43}$$

### 5.3.2 Solution of the first-order system

From Eqs. (5.31) and (5.42), the zero[th] order axial velocity of the solid particles is given by

$$u_p{}^{(0)} = \frac{P_0}{4} \left( r^2 - h^2 - \frac{4}{M} \right). \tag{5.44}$$

Integrating continuity equation (5.29) together with Eq. (5.44) with respect to $r$ and using the first boundary condition of (5.32), the zero[th] order radial velocity of the particle is obtained as

$$v_p{}^{(0)} = \frac{r}{4} \left\{ P_0 h \frac{\partial h}{\partial x} - \frac{\partial P_0}{\partial x} \left( \frac{r^2}{4} - \frac{h^2}{2} - \frac{2}{M} \right) \right\}. \tag{5.45}$$

Equations (5.26)-(5.28) of the first order system are solved similarly as described in the solution of zeroth order system.

The first order solutions for the axial and radial velocities of the fluid (the details are given in the Appendix 5.A) are given by

$$u_f{}^{(1)} = N_1(r^6 - h^6) + N_2(r^4 - h^4) + \left(N_3 + \frac{P_1 + C^{(1)}P_0}{4}\right)(r^2 - h^2). \tag{5.46}$$

$$v_f{}^{(1)} = -\frac{1}{8}\frac{\partial N_1}{\partial x}(r^7 - 4h^6 r) - \frac{1}{6}\frac{\partial N_2}{\partial x}(r^5 - 3rh^4) - \frac{1}{4}\left(\frac{\partial N_3}{\partial x} + \frac{1}{4}\frac{\partial P_1}{\partial x} + \frac{C^{(1)}}{4}\frac{\partial P_0}{\partial x}\right)(r^3 - 2rh^2) + \frac{1}{4}\left(12N_1 + 8N_2h^3 + 2N_3h + P_1h + P_0hC^{(1)}\right)\frac{\partial h}{\partial x}r. \tag{5.47}$$

The expressions for $P_1, N_1, N_2$ and $N_3$ are given by

$$P_1 = \frac{\partial p^{(1)}}{\partial x} = -6N_1h^4 - \frac{16}{3}N_2h^2 - 4N_3 - \frac{P_0C^{(1)}}{h^2}\left(\frac{8}{M} + h^2\right) - \frac{8\bar{Q}^{(1)}}{h^4}, \tag{5.48}$$

where

$$N_1 = \frac{Re_0}{1152}P_0\frac{\partial P_0}{\partial x}. \tag{5.49}$$

$$N_2 = \frac{Re_0}{16}\left(\frac{1}{3}\frac{\partial P_0}{\partial t} - \frac{3P_0}{8}\frac{\partial P_0}{\partial x}h^2\right). \tag{5.50}$$

$$N_3 = Re_0\left(\frac{h^2}{12}\frac{\partial P_0}{\partial t} - \frac{P_0}{8}\frac{\partial h}{\partial t}h + \frac{3P_0}{32}\frac{\partial P_0}{\partial x}h^4 + \frac{P_0^2h^3}{32}\frac{\partial h}{\partial x}\right), \tag{5.51}$$

and $\bar{Q}^{(1)} = Q^{(1)} = -\frac{3}{4}N_1h^8 - \frac{2}{3}N_2h^6 - \left(\frac{N_3}{2} + \frac{1}{8}\frac{\partial p^{(1)}}{\partial x} + \frac{P_0C^{(1)}}{8}\right)h^4 - \frac{P_0C^{(1)}}{M}h^2$ (see Appendix 5.B)

The zero[th] and first order solutions of those given in Eqs. (5.17)-(5.20), together constitute the required results for the fluid and particle velocities. Therefore, the axial and radial velocities of the fluid in the fixed frame are

$$u_f = \frac{P_0}{4}(r^2 - h^2) + \delta\left\{N_1(r^6 - h^6) + N_2(r^4 - h^4) + \left(N_3 + \frac{P_1 + C^{(1)}P_0}{4}\right)(r^2 - h^2)\right\}. \tag{5.52}$$

$$v_f = \frac{r}{4}\left\{h\frac{\partial h}{\partial x}P_0 - \frac{\partial P_0}{\partial x}\left(\frac{r^2}{4} - \frac{h^2}{2}\right)\right\} + \delta\left\{-\frac{1}{8}\frac{\partial N_1}{\partial x}(r^7 - 4h^6r) - \frac{1}{6}\frac{\partial N_2}{\partial x}(r^5 - 3rh^4) - \frac{1}{4}\left(\frac{\partial N_3}{\partial x} + \frac{1}{4}\frac{\partial P_1}{\partial x} + \frac{C^{(1)}}{4}\frac{\partial P_0}{\partial x}\right)(r^3 - 2rh^2) + \frac{1}{4}\left(12N_1 + 8N_2h^3 + 2N_3h + P_1h + P_0hC^{(1)}\right)\frac{\partial h}{\partial x}r\right\}. \tag{5.53}$$

### 5.3.3 Pressure gradient

The perturbation expansion for pressure gradient is

$$\frac{\partial p}{\partial x} = \frac{\partial p^{(0)}}{\partial x} + \delta \frac{\partial p^{(1)}}{\partial x} + O(\delta^2).$$

Therefore, the solution for pressure gradient in terms of time-averaged volume flow rate, in view of Eqs. (5.41) and (5.48), yields

$$\frac{\partial p}{\partial x} = -8\left(\frac{\bar{Q}^{(0)} - 1 + \emptyset\, e^{kx} - \frac{3}{8}\emptyset^2 e^{2kx} + h^2}{h^4}\right) - \delta\left\{6N_1 h^4 + \frac{16}{3}N_2 h^2 + 4N_3 - 8C^{(1)}\left(\frac{\bar{Q}^{(0)} - 1 + \emptyset\, e^{kx} - \frac{3}{8}\emptyset^2 e^{2kx} + h^2}{h^6}\right)\left(\frac{8}{M} + h^2\right) + \frac{8\bar{Q}^{(1)}}{h^4}\right\}. \quad (5.54)$$

### 5.3.4 Stream function

The flow patterns of fluid are also given by counters of the constant stream function, $\Psi_f$, in the moving frame defined as

$$d\Psi_f = 2RU_f dR - 2RV_f dX.$$

Using the transformation defined in Eq. (5.34), the stream function, $\psi_f(r, x, t)$, in the fixed frame may be obtained by the solution of the differential equation, $d\psi_f = 2r\left(u_f - 1\right)dr - 2rv_f dx$. This is an exact differential equation; therefore stream function may be obtained by evaluating

$$2\int\left[\frac{P_0}{4}(r^2 - h^2) + \delta\left\{N_1(r^6 - h^6) + N_2(r^4 - h^4) + \left(N_3 + \frac{P_1 + C^{(1)}P_0}{4}\right)(r^2 - h^2)\right\} - 1\right] r dr.$$

Thus we have

$$\psi_f(r, x, t) = r^2\left[\frac{P_0}{8}(r^2 - 2h^2) + \delta\left\{\frac{N_1}{4}(r^6 - 4h^6) + \frac{N_2}{3}(r^4 - 3h^4) + \frac{1}{8}\left(4N_3 + P_1 + C^{(1)}P_0\right)(r^2 - 2h^2)\right\} - 1\right]. \quad (5.55)$$

For wave number, $\delta \to 0$, Eqs. (5.52)-(5.55) reduce to the corresponding equations derived by Shapiro et al. (1969).

## 5.4 Discussions and results

In order to have an estimate of applicability of the analytical work presented here, we consider the length and the diameter of the oesophagus as 25-30 cm (Lamb and Griffin, 2005) and 1.8-2.1 cm (Joohee et al., 2012) respectively. Suspended particles have uniform radii $0.04$ cm.We also consider that oesophagus can contain two boluses at a time while swallowing.

With these dimensions of the oesophagus, the following parameters are evaluated as $\delta = 0.06$ and $M = 1139$. The analytical results are expressed in the fixed frame up to the first order of the time-averaged volume flow rate $\bar{Q} = \bar{Q}^{(0)} + \delta\bar{Q}^{(1)}$. Then computer codes are developed by substituting $\bar{Q}^{(0)} = \bar{Q} - \delta\bar{Q}^{(1)}$ in the solutions (5.52)-(5.55) for numerical evaluations of the analytical results. Diagrams are drawn for the pressure gradient, the axial and radial velocities and the streamlines of the flow shown in Figs. 2-8 with various parameters as assumed below.

The axial velocity of the fluid together with that of the solid particles along the axis of the oesophagus is presented in Fig. 5.2 at the fixed radial distance $r = 0.3$ and the temporal values (a) $t = 0.0$ (b) $t = 0.4$ . This figure is based on Eqs. (5.44) and (5.52). Other parameters are taken as $\delta = 0.06, k = 0.02, C = 0.12,\ \emptyset = 0.7,\ Re_0 = 5, \bar{Q} = 1.5, \bar{Q}^{(1)} = 15,\ M = 1139$. At $t = 0.0$ (Fig. 5.2a), we observe that the axial velocity of the fluid is greater than that of the solid particles almost everywhere. But analyzing Eqs. (5.44) and (5.52), we infer that at the wall the axial velocity of the fluid is zero but the suspended particulate material has non-zero positive axial velocity. This means that the axial velocity of the suspended particles near the tube wall is more than that of the fluid velocity. It has been illustrated in Fig. 5.3 by plotting graphs of the axial velocities close to the tube wall. In Fig. 5.2b, we also observe that the axial velocity is negative in the regions close to maximum occlusions giving way to instantaneous backward flow. Backward flow is found in a small region with maximum occlusion. Therefore, the net flow will be positive. Further, it is observed that the magnitude of the velocity at the second occlusion point is more than at the first occlusion point which is due to dilating wave amplitude.

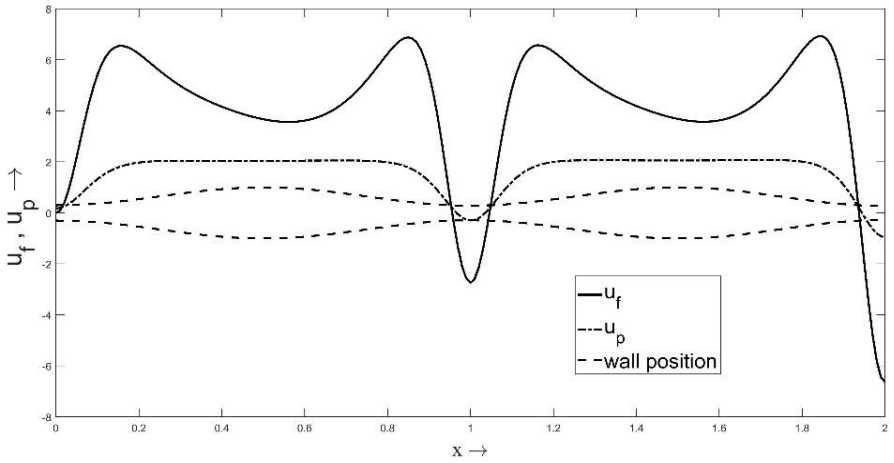


(a) $t = 0.0$

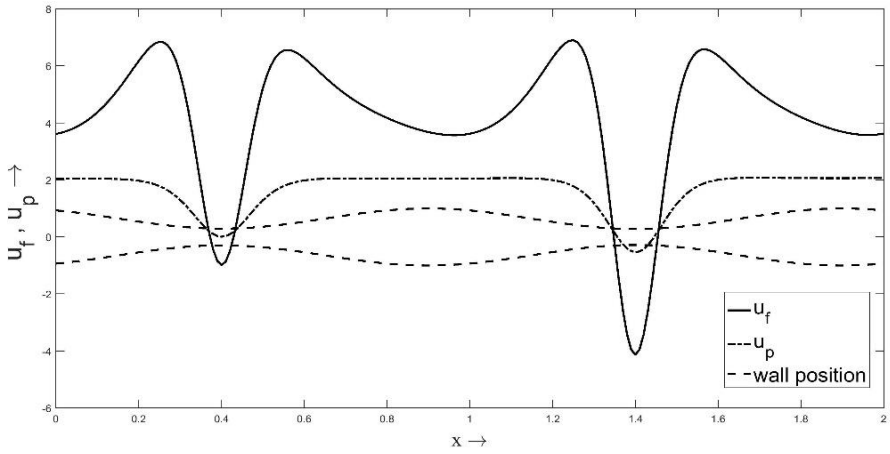


(b) $t = 0.4$

***Fig. 5.2***(a-b) *Axial velocity profile of the fluid and solid particles versus the tube length at the fixed radial distance* $r = 0.3$ *and* (a) $t = 0.0$ (b) $t = 0.4$ *. Other parameters are taken as* $\delta = 0.06,\ k = 0.02,\ C = 0.12,\ \emptyset = 0.7,\ Re_0 = 5,\ \bar{Q} = 1.0, \bar{Q}^{(1)} = 15,\ M = 1139$ .

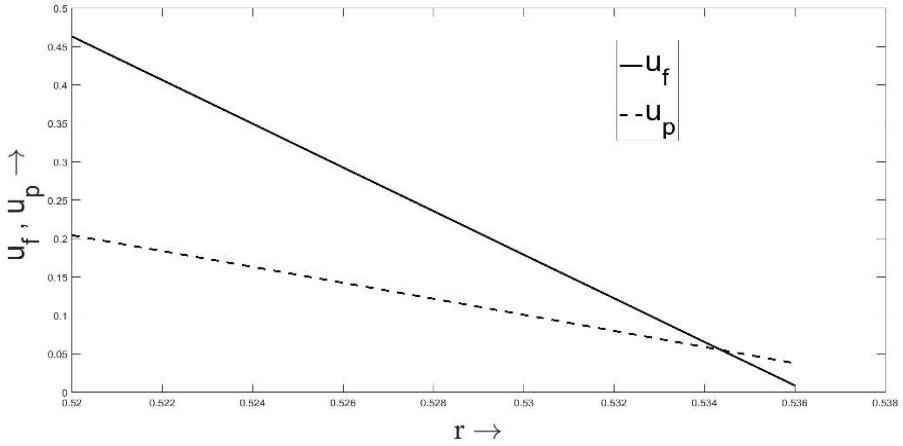


***Fig. 5.3*** *The radial profiles of the axial velocity respectively of the fluid and solid particles versus the tube radius at the fixed axial position* $x = 0.6$ *and* $t = 0.4$*. Other parameters are taken as* $\delta = 0.06,\ k = 0.02,\ C = 0.12,\ \emptyset = 0.7,\ Re_0 = 5,\ \bar{Q} = 1.5, \bar{Q}^{(1)} = 20,\ M = 1139$ .

The impact of dilating wave amplitude on the axial velocity is depicted in Fig. 5.4 in which the various parameters are taken as $k = 0.0,\ 0.05,\ 0.1,\ x = 0.3,\ t = 0.9,\ \delta = 0.06,\ C = 0.12,\ \emptyset = 0.7,\ Re_0 = 5,\ \bar{Q} = 1.5,\ \bar{Q}^{(1)} = 20,\ M = 1139$. It is observed that the greater the dilation parameter, the higher is the axial velocity at the fixed axial positions for both the fluid and particles velocities.

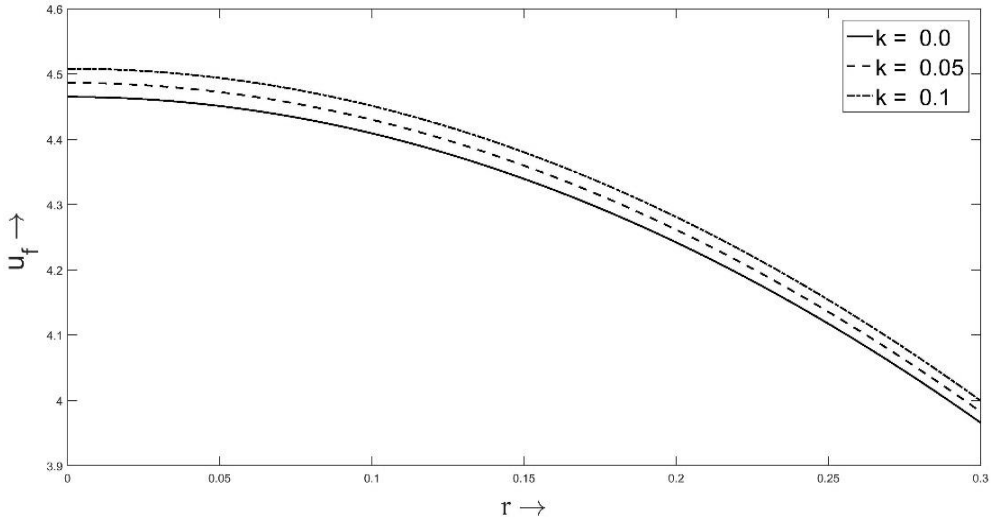


(a)

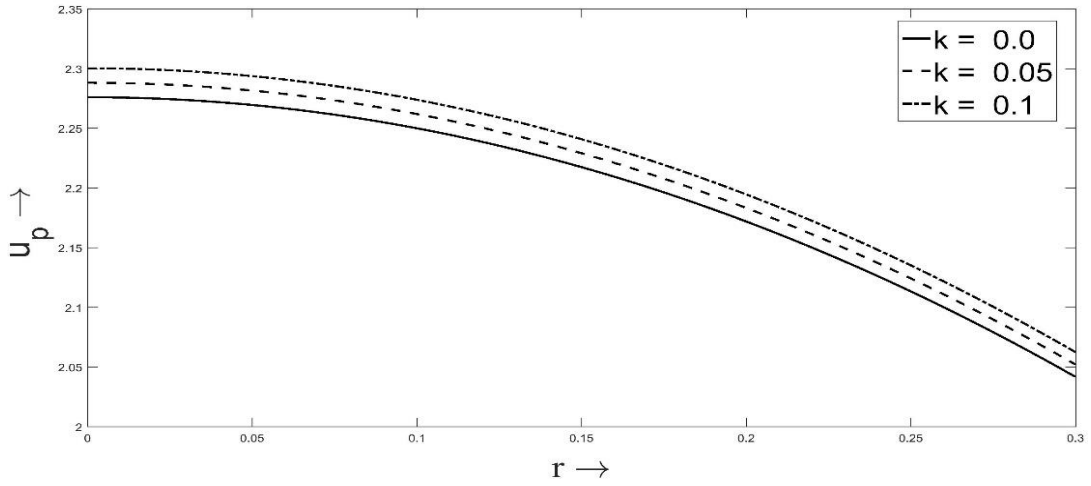


(b)

***Fig. 5.4***(a-b) *Radial profiles the axial velocity respectively of* (a) *the fluid and* (b) *solid particles versus the radial distance at the fixed axial position* $x = 0.3$ *and time* $t = 0.9$ *showing the impact of amplitude dilation parameter* $k$*. Other parameters are taken as* $\delta = 0.06,\ C = 0.12,\ \emptyset = 0.7,\ Re_0 = 5,\ \bar{Q} = 1.5, \bar{Q}^{(1)} = 20,\ M = 1139$ *. Solid, dashed and dashed dotted line correspond respectively to* $k = 0.0,\ k = 0.05$ *and* $k = 0.1$*.*

Figure 5.5(a) illustrates the impact of the particulate suspension on the axial velocity of the fluid along the radius at a specific axial location $x = 0.3$ and at an instant $t = 0.9$ comprising three distinct curves for different volume fractions $C = 0.0,\ 0.12,\ 0.24$. We take other parameters as $k = 0.02,\ \emptyset = 0.8,\ Re_0 = 5,\ \bar{Q}^{(1)} = 20$. Examining the behaviour of the present figure, we observe that the axial velocity of the fluid decreases with increasing volume fraction. The curves are all analogous in the sense that they decrease from their individual maximum at the axis to the minimum near the wall surface as expected. We draw another graph for the axial fluid velocity with the same parameters as in Fig. 5.5(a) except for $\delta = 0$, i.e., particle-free fluid which is shown in Fig. 5.5(b). Comparing Figs. 5.5(a) and 5.5(b), we find that the maximum axial velocity of particle-fluid suspension with non-zero wave number is more than that of particle-free fluid with zero wave number.

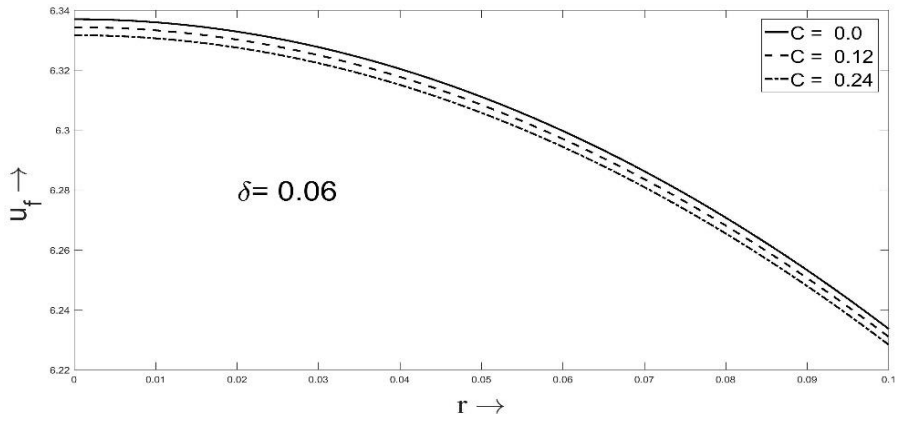


(a)

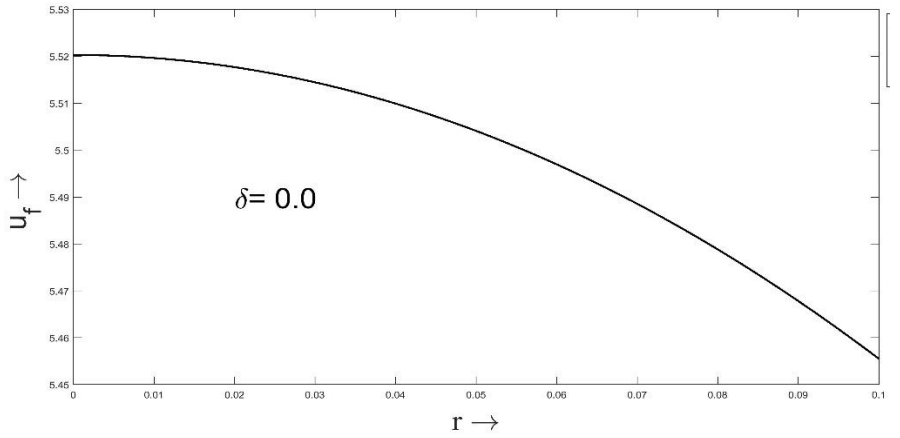


(b)

***Fig. 5.5***(a-b) *The impact of $\delta$ on the relation between the axial velocity of the fluid and the radial distance for different volume fractions at the fixed axial position $x = 0.3$ for $k = 0.02, \emptyset = 0.8, Re_0 = 5,\ \bar{Q} = 1.5, \bar{Q}^{(1)} = 20,\ t = 0.9,\ M = 1139,$* (a) $\delta = 0.06$, (b) $\delta = 0.0$. *Solid line, dashed line and dashed dotted line respectively correspond to $C = 0.0,\ C = 0.12$ and $C = 0.24$.*

The characteristics of the radial velocity of the fluid varying radially at the fixed axial position $x = 0.2$ for $t = 0.3$ and different volume fractions ($C = 0.0,\ 0.12,\ 0.24$) are exhibited in Fig. 5.6. Analyzing all the curves of the depicting figure, we see that all the curves diminish from zero on the axis as these move away from it and finally move towards the wall to attain some finite value on the wall surface. These natures of curves reflect the presence of wall motion in the transverse direction. It is interesting to see that all the curves become concave near the wall which means that the radial velocity changes its nature near

the wall. A rise in the volume fraction of suspended particles diminishes the magnitude of the radial velocity of the fluid.

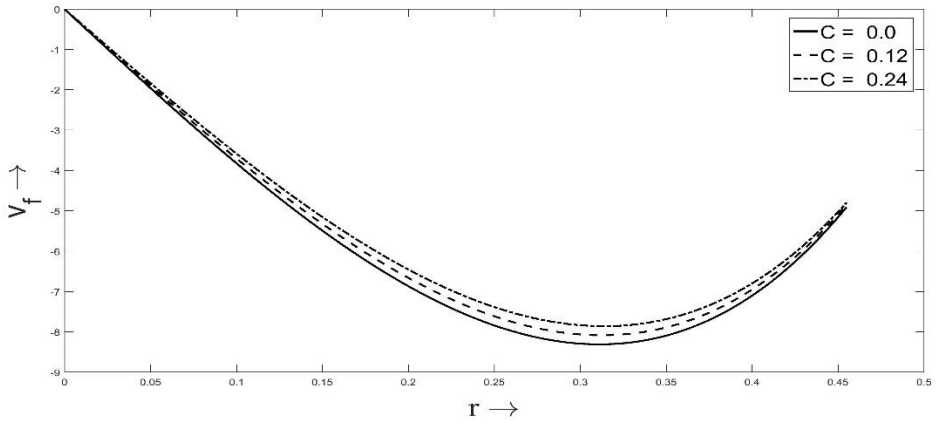


***Fig. 5.6*** *Radial velocity profile of the fluid along the radial distance for different volume fraction of particles at* $x = 0.2$ *for* $t = 0.3$, $k = 0.02, \emptyset = 0.6, Re_0 = 5$, $\delta = 0.06, \bar{Q} = 1.5$, $\bar{Q}^{(1)} = 20, M = 1139$. *Solid line, dashed line and dashed dotted line correspond respectively to* $C = 0.0$, $C = 0.12$ *and* $C = 0.24$.

Figure 5.7(a) displays the pressure gradient of the fluid-particle mixture versus the time-averaged volume flow rate $\bar{Q}$ for different volume fractions ($C = 0.0,\ 0.12,\ 0.24$) at the fixed axial position and the fixed time. We randomly choose the axial position $x = 0.8$ and the time $t = 0.4$ . For the qualitative interpretation of the analytical result we take other parameters as $k = 0.02,\ \emptyset = 0.6,\ Re_0 = 5,\ \bar{Q}^{(1)} = 15$. A close observation reveals that as the volume fraction increases from 0.0 to 0.24, the pressure gradient too declines. This means that the dispersed small particles in the fluid medium affect the pumping characteristics. It is also observed that below some fixed flow rate, the pressure gradient is adverse, i.e. $\frac{\partial p}{\partial x} > 0$; but above that the pressure gradient is favorable, i.e. $\frac{\partial p}{\partial x} < 0$. It is inferred that a positive pressure gradient hinders the flow while a negative one enhances it. In Fig. 5.7(b), $\frac{\partial p}{\partial x}$ vs. $\bar{Q}$ is also plotted under the same condition as in Fig. 5.7(a) but at the wave number, $\delta = 0$. Comparing Fig. 5.7(b) with 5.7(a), we note that the pressure gradient varies linearly with the volume flow rate in Fig. 5.7b but not in Fig. 5.7(a). The reason behind this is that the expressions defined by $N_1,\ N_2$ and $N_3$ contain quadratic terms in $\bar{Q}$ but when $\delta = 0$, these terms are absent in the pressure gradient and only the linear term of $\bar{Q}$ is left.

There are several diseases like achalasia, oesophageal stricture and oesophageal tumors in which swallowing is very difficult. Pressure gradient profile suggests that patients suffering from these diseases may be advised to consume food items with less particulate suspensions. Larger pressure gradient for low volume fraction is advised for comfortable swallowing.

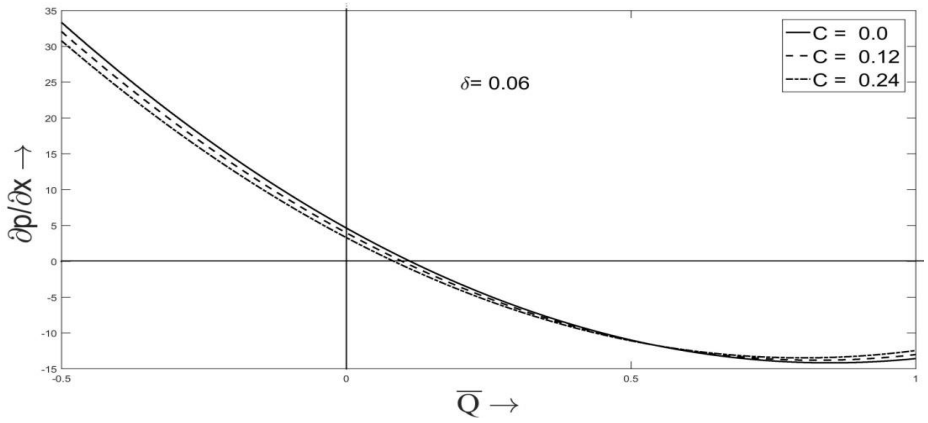


(a)

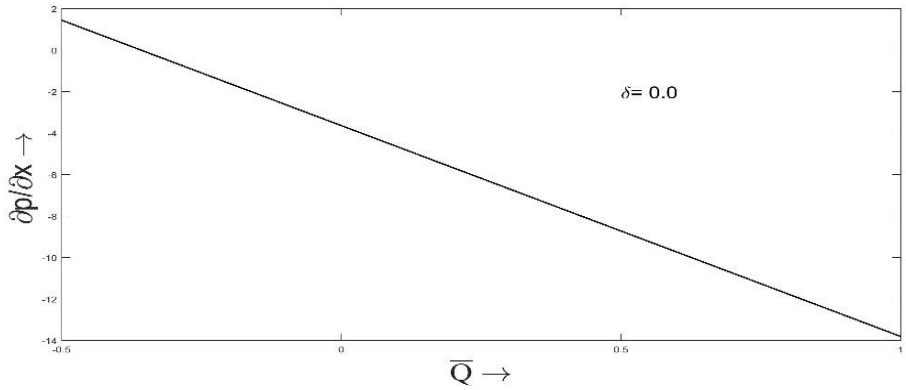


(b)

***Fig. 5.7***(a-b) *The effect of $\delta$ on the relation between the pressure gradient and the time-averaged volume flow rate for different volume fraction of particles with $k = 0.02,\ \emptyset = 0.6,\ Re_0 = 5,\ \bar{Q}^{(1)} = 15,\ M = 1139,\ x = 0.8,\ t = 0.4$, (a) $\delta = 0.06$, (b) $\delta = 0.0$ Solid line, dashed line and dashed dotted line correspond to $C = 0.0$, $C = 0.12$ and $C = 0.24$ respectively.*

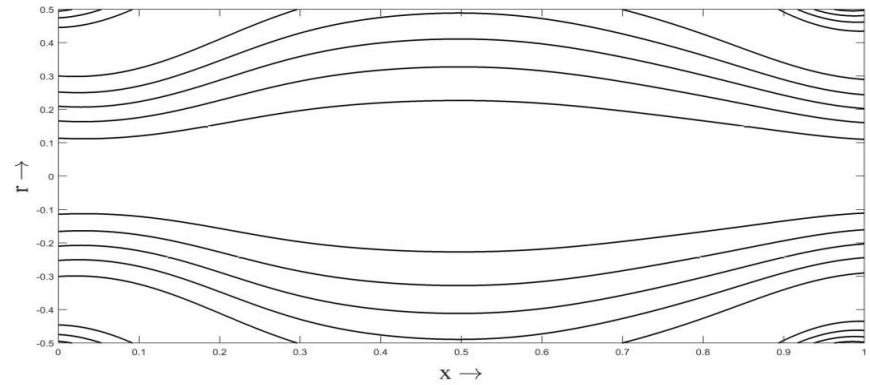


(a)

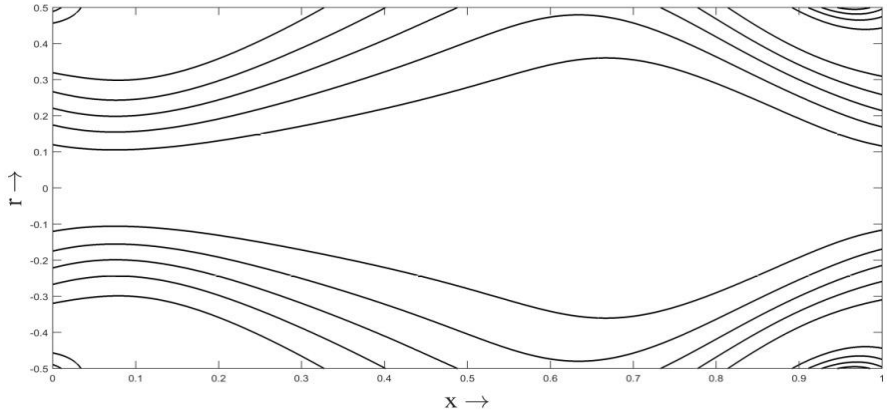


(b)

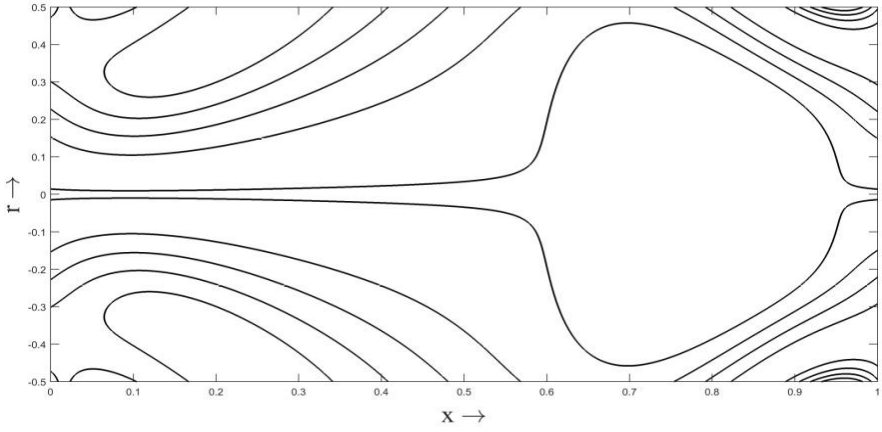


(c)

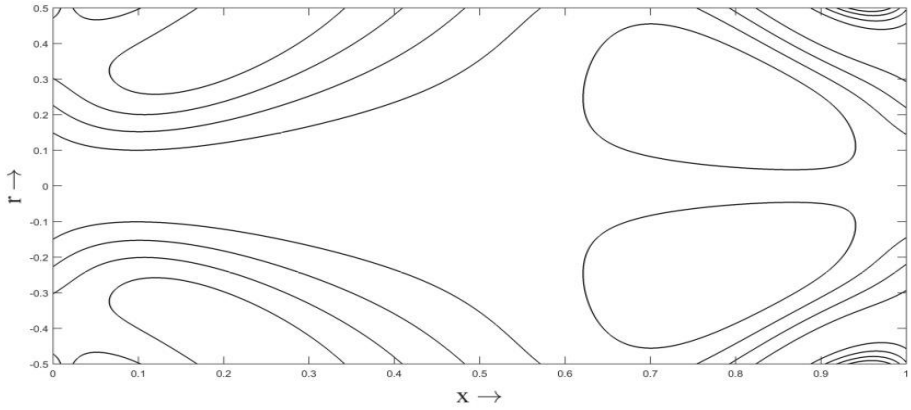


(d)

***Fig. 5.8***(a-d) *Streamlines in the fixed frame with* $k = 0.02,\ C = 0.12,\ \emptyset = 0.6,\ Re_0 = 5,\ \delta = 0.06, \bar{Q}^{(1)} = 20,\ M = 1139,\ t = 1.0$ *at different time-averaged volume flow rates* (a) $\bar{Q} = 1.2$, (b) $\bar{Q} = 3.2$, (c) $\bar{Q} = 5.0$ *and* (d) $\bar{Q} = 5.1$.

The fluid motion is also described with the help of streamlines and stream functions. A streamline is an imaginary curve in the flow field of the fluid such that the tangent at each of the points of the curve gives the direction of the local velocity at that point at an instant. Streamlines in the fixed frame with $k = 0.02,\ \emptyset = 0.6,\ Re_0 = 5,\ \delta = 0.06,\ \bar{Q}^{(1)} = 20,\ M = 1139,\ t = 1.0$ at different time-averaged volume flow rates ($\bar{Q} = 1.2\,,\ 3.2,\ 5.0,\ 5.1$) are shown in Fig. 5.8. A close look of this figure reveals that the fluid streamlines are generally similar to the shape of the wall for small $\bar{Q}$ (Fig. 5.8a). Another observation is that when $\bar{Q}$ is increased, the streamlines change its shape and above a certain $\bar{Q}$, the central streamline splits to engulf a ring-shaped bolus of the fluid as a closed streamline as depicted in Figs. 5.8(b)-(d). This trapped bolus is now pushed ahead along with the peristaltic wave. This leads us to infer that trapping takes place at high flow rates. This phenomenon, termed as trapping, was first discovered by Shapiro et al. (1969).

## 5.5 Conclusions

Peristaltic transport of particle-fluid suspension through oesophagus is investigated theoretically by regular perturbation technique. The impact of volume fraction of particles on the pressure gradient and the velocity is examined and streamline patterns are obtained. The presence of particles affects the pumping performance and velocity.

It is observed that the axial velocity of the fluid is greater than that of the solid particles almost everywhere. However, at the wall the axial velocity of the fluid is zero due to the no-slip condition imposed on it; but the suspended particulate material has non-zero positive axial velocity. Thus, that the axial velocity of the suspended particles near the tube wall is more than that of the fluid velocity. It is further observed that the axial velocity is negative in the regions close to maximum occlusions giving way to instantaneous backward flow. Backward flow is created in a small region with maximum occlusion. Hence, the net flow will be positive. Further, the magnitude of the velocity at the second occlusion point is more than at the first occlusion point which is due to dilating wave amplitude.

It is also inferred that that the maximum axial velocity of particle-fluid suspension with non-zero wave number is more than that of particle-free fluid with zero wave number.

An increment in volume fraction of suspended particles diminishes the pressure gradient and hence also the axial and radial velocities. The research endorses the advice of the doctors to the patients suffering from achalasia, oesophageal stricture and oesophageal tumors to consume liquid or food items with lesser solid contents.

Streamline patterns are changed by increasing flow rate while trapping occurs at high flow rates.

**Appendix 5.A**

Using Eqs. (5.42) and (5.44) in Eq. (5.28), we have

$$Re_0\left[\frac{1}{4}\frac{\partial P_0}{\partial t}(r^2-h^2)-\frac{hP_0}{2}\frac{\partial h}{\partial t}+\left\{\frac{rhP_0}{4}\frac{\partial h}{\partial x}-\frac{r}{16}\frac{\partial P_0}{\partial x}(r^2-2h^2)\right\}\frac{rP_0}{2}+\frac{P_0}{4}(r^2-h^2)\left\{\frac{1}{4}\frac{\partial P_0}{\partial x}(r^2-h^2)-\frac{hP_0}{2}\frac{\partial h}{\partial x}\right\}\right]=-\frac{\partial p^{(1)}}{\partial x}+\frac{1}{r}\frac{\partial}{\partial r}\left(r\frac{\partial u_f^{(1)}}{\partial r}\right)+MC^{(1)}\left\{\frac{P_0}{4}\left(r^2-h^2-\frac{4}{M}\right)-\frac{P_0}{4}(r^2-h^2)\right\}. \quad (5.A1)$$

Integrating Eq. (5.A1) with respect to $r$ and using the second boundary condition of Eq. (5.32), we get

$$\frac{\partial u_f^{(1)}}{\partial r}=\frac{r}{2}\frac{\partial p^{(1)}}{\partial x}+\frac{rP_0C^{(1)}}{2}+Re_0\left\{\frac{1}{16}\frac{\partial P_0}{\partial t}(r^3-2h^2r)-\frac{rhP_0}{4}\frac{\partial h}{\partial t}+\frac{rh^3P_0^2}{16}\frac{\partial h}{\partial x}+\frac{P_0}{384}\frac{\partial P_0}{\partial x}(2r^5-6h^3r^3+12rh^4)\right\}. \quad (5.A2)$$

Integrating Eq. (5.A2) with respect to $r$ and using the third boundary condition of Eq. (5.32), we obtain ${u_f}^{(1)}$ given in Eq. (5.46). Further, using Eq. (5.46) in Eq. (5.26) and integrating it with respect to $r$ under the fifth boundary condition of Eq. (5.32), we get ${v_f}^{(1)}$ given by Eq. (5.47).

**Appendix 5.B**

In view of Eq. (5.33), the first order volume flow rate in the fixed frame is $Q^{(1)} = Q_f^{(1)} + Q_p^{(1)}$, where $Q_f^{(1)} = 2\int_0^h {u_f}^{(1)} r dr - 2C^{(1)} \int_0^h {u_f}^{(0)} r dr$ and $Q_p^{(1)} = 2C^{(1)} \int_0^h {u_p}^{(0)} r dr$ . Therefore, using Eqs. (5.42), (5.44) and (5.46), we derive the first order volume flow rate as

$$Q^{(1)} = -\frac{3}{4} N_1 h^8 - \frac{2}{3} N_2 h^6 - \left(\frac{N_3}{2} + \frac{1}{8}\frac{\partial p^{(1)}}{\partial x} + \frac{P_0 C^{(1)}}{8}\right) h^4 - \frac{P_0 C^{(1)}}{M} h^2. \qquad (5.B1)$$

In view of Eq. (5.35), it is also noted that the first order time averaged volume flow rate, $\bar{Q}^{(1)} = Q^{(1)}$.